J Wood Sci (2017) 63:253–262
DOI 10.1007/s10086-017-1622-7

ORIGINAL ARTICLE

Effects of climate change on reduction of internal bond strength of particleboard subjected to various climatic conditions in Japan

Hideaki Korai[1] · Katsuhiro Nakao[1] · Tetsuya Matsui[1] · Ken Watanabe[1] · Yasushi Ishigooka[2]

Received: 1 November 2016 / Accepted: 21 February 2017 / Published online: 6 April 2017

Abstract The effects of climate change on the reduction of internal bond strength (IB) of particleboard subjected to various climatic conditions in Japan were predicted. The temperature increased throughout Japan with increasing greenhouse gas (GHG) emissions, so the climate deterioration index (climate index for predicting the IB reduction of particleboard; a high index indicates a large IB reduction) also increased to decrease IB. The number of low-temperature areas decreased because of climate change. The rupture of bonding points in particleboard caused by outdoor exposure led to a IB reduction, and biodeterioration accelerated this reduction. In high-temperature areas, particleboard was found to be prone to biodeterioration, and the IB significantly reduced. An area wherein there was a significant decrease in the IB spread along the Pacific Ocean side of western Japan and the Sea of Japan in central Japan in relation to increasing GHG emissions. Particleboards are difficult to use outdoors because of climate change.

Keywords Particleboard · Outdoor exposure · Climate change · Climatic condition · Internal bond strength

Introduction

Particleboard is typically used indoors only, but its use needs to be extended outdoors to create an increased demand for the product. Thus, the effect of outdoor exposure on particleboard must be investigated. Although outdoor exposure tests have been conducted on particleboard in North America [1–3], very few tests were conducted in Japan until the early 2000s [4]. Therefore, eight sites that are representative of the Japanese climate were selected, and particleboard was subjected to various climatic conditions from 2004 to 2011 by the Research Working Group on Wood-based Panels of the Japan Wood Research Society. The sites were Asahikawa, Noshiro, Morioka, Tsukuba, Maniwa, Okayama, Shizuoka, and Miyakonojo, which are numbered from 1 to 8, respectively, in Table 1. The results of this research group were recently reported in the following papers, e.g. [5–8].

With regard to the effects of climatic conditions on the strength reduction of particleboard, Kojima et al. [7] reported that temperature, sunshine duration, and precipitation are important factors. In our previous study [9, 10], these three climatic conditions were combined into the first principal component (PC1) in principal component analysis (PCA), and the first principal component score (PC1 score) was closely related to the strength reduction of particleboard. Results showed that the strength of particleboard subjected to outdoor exposure in high-PC1 score areas reduced significantly. Therefore, the PC1 score was determined to be an effective index for predicting strength reduction resulting from outdoor exposure, and it was named the "climate deterioration index (CDI)".

In general, climate change causes serious problems, and many researchers have predicted effects on human life. In this study, the effects of climate change on the reduction of internal bond strength (IB) of particleboard subjected to various climatic conditions in Japan were predicted. Anthropogenic greenhouse gas (GHG) emissions are mainly driven by population size, economic activity,

✉ Hideaki Korai
korai@ffpri.affrc.go.jp

[1] Forestry and Forest Products Research Institute, Tsukuba 305-8687, Japan

[2] Institute for Agro-Environmental Sciences, Tsukuba 305-8604, Japan

Table 1 Site numbers, sites, north latitude, east longitude, and temperature grouping at outdoor exposure sites

Site no.	Site	Third mesh code	North latitude	East longitude	Temperature grouping
1	Asahikawa	65424330	43°41′	142°22′	Low
2	Noshiro	60402020	40°11′	140°00′	Low
3	Morioka	59413047	39°37′	141°05′	Low
4	Tsukuba	54400048	36°02′	140°05′	Middle
5	Maniwa	52335505	35°05′	133°41′	Middle
6	Okayama	52330622	34°41′	133°46′	High
7	Shizuoka	52383354	34°57′	138°25′	High
8	Miyakonojo	47314076	31°43′	131°05′	High

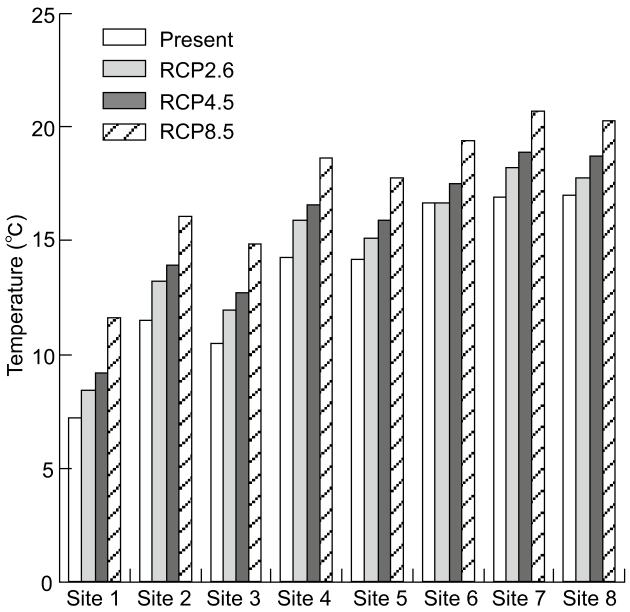

Fig. 1 Temperature change in compliance with three RCP scenarios, i.e., RCP2.6, RCP4.5, and RCP8.5, at eight sites. *RCP* representative concentration pathway. Details about the sites are provided in Table 1

lifestyle, energy use, land use patterns, technology, and climate policy. The representative concentration pathways (RCPs), which are used to make projections in this study based on these factors, describe four 21st century pathways for GHG emissions and atmospheric concentrations, air pollutant emissions, and land use [11]. The RCPs involved are a stringent mitigation scenario (RCP2.6), two intermediate scenarios (RCP4.5 and RCP6.0), and one scenario with very high GHG emissions (RCP8.5) [11]. Scenarios without additional efforts to constrain emissions ('baseline scenarios') lead to pathways ranging between RCP6.0 and RCP8.5. RCP2.6 is representative of a scenario that aims to keep global warming below 2 °C above pre-industrial temperatures [11]. Figure 1 shows temperature change in compliance with the three RCP scenarios (RCP2.6, RCP4.5, and RCP8.5) at the eight sites. Temperature change of even the RCP2.6 has widespread impacts on the eight sites. In this study, the CDI was predicted for 2031–2050 using three RCP scenarios (RECP2.6, RCP4.5, and RCP8.5). The effects of climate change on the IB reduction of particleboard subjected to various climatic conditions in Japan were predicted using the CDI based on the three RCP scenarios.

Experimental

Outdoor exposure and IB tests

Particleboard was subjected to outdoor exposure at eight sites from February 2004 to March 2009. The sites are listed in Table 1, wherein the small numbers indicate northern sites. In general, temperature plays an important role to reduce IB, and the eight sites were classified as low-, middle-, and high-temperature sites (Table 1). The annual climatic conditions of mean temperature, solar radiation, and precipitation at these sites are listed in Table 2.

In this study, commercially available phenol–formaldehyde resin-bonded particleboard was used, which has a thickness and density of 12.2 mm and 0.75 g/cm^3, respectively. Thirty to forty particleboards measuring 910 mm × 1823 mm were cut into specimens measuring 300 mm × 300 mm. Specimens were selected at random and subjected to outdoor exposure vertically to the south at each site, as shown in Fig. 2. The IB test was conducted in compliance with JIS [13], and the IB data have reported previously [6, 9, 10, 14]. The mean and standard deviation of the initial IB were 0.833 and 0.09 MPa, respectively.

PCA using climatic conditions at eight sites

PCA was conducted using computer software "R. 3.0.2" [15]. Table 2 lists the temperature, precipitation, and solar

Table 2 Climatic conditions and IB at outdoor exposure sites from April 2004 to March 2009

Outdoor exposure time (year)	Site no.	Climatic conditions			CDI	IB (MPa)	
		T (°C)	P (mm)	S (MJ/m^2)		Mean	SD
1	1	7.2	984	11.9	−2.15	0.812	0.07
	2	11.6	1731	**10.6**	−1.48	0.630	0.10
	3	10.6	1535	12.2	−1.12	0.639	0.09
From April 2004	4	14.5	1693	14.0	0.348	0.605	0.09
to March 2005	5	14.5	1683	**12.4**	−0.300	0.551	0.10
	6	16.9	1509	**14.2**	0.716	0.556	0.07
	7	17.4	3454	14.4	2.08	0.337	0.15
	8	16.9	3302	**14.4**	1.91	0.229	0.04
2	1	7.0	987	11.9	−2.09	0.626	0.05
	2	11.4	1622	**10.6**	−1.39	0.540	0.16
	3	10.3	1468	12.2	−1.04	0.458	0.11
From April 2004	4	14.2	1409	14.0	0.325	0.573	0.22
to March 2006	5	14.2	1355	**12.4**	−0.374	0.434	0.14
	6	16.7	1141	**14.2**	0.632	0.324	0.17
	7	17.0	2624	14.4	1.88	0.212	0.11
	8	16.8	2889	**14.4**	2.05	0.125	0.07
3	1	7.1	1009	11.8	−2.16	0.666	0.10
	2	11.5	1571	**10.8**	−1.35	0.464	0.12
	3	10.4	1370	12.3	−1.07	0.521	0.14
From April 2004	4	14.3	1455	13.7	0.274	0.318	0.13
to March 2007	5	14.2	1326	**12.5**	−0.372	0.323	0.13
	6	16.7	1160	**14.3**	0.685	0.185	0.11
	7	17.0	2432	14.3	1.84	0.152	0.06
	8	17.0	2688	**14.5**	2.15	0.092	0.04
4	1	7.1	966	12.0	−2.09	0.596	0.13
	2	11.5	1475	**11.2**	−1.28	0.287	0.12
	3	10.4	1348	12.3	−1.02	0.480	0.14
From April 2004	4	14.3	1377	13.4	0.219	0.320	0.19
to March 2008	5	14.2	1315	**12.0**	−0.565	0.186	0.07
	6	16.7	1082	**14.0**	0.653	0.208	0.12
	7	16.9	2326	14.0	1.84	0.069	0.03
	8	17.0	2569	**14.3**	2.24	0.057	0.02
5	1	7.2	946	12.0	−2.13	0.360	0.25
	2	11.5	1470	**11.3**	−1.29	0.377	0.15
From April 2004	3	10.5	1315	12.4	−1.01	0.193	0.11
to March 2009	4	14.3	1399	13.3	0.204	0.140	0.11
	5	14.2	1274	**12.2**	−0.524	0.119	0.10
	6	16.7	1057	**14.0**	0.680	0.186	0.08
	7	16.9	2302	14.0	1.85	0.054	0.02
	8	17.0	2566	**14.2**	2.22	0.056	0.02

Details about the sites are provided in Table 1. Due to a lack of climatic conditions for Site 5 (Maniwa), the conditions for Tsuyama (located near Maniwa) were used. Boldface indicates solar radiation predicted using model that was developed by Kondo [12]

T annual mean temperature, *P* annual precipitation, *S* annual solar radiation, *CDI* climate deterioration index (first principal component score), *IB* internal bond strength, *SD* standard deviation

radiation at the eight sites recorded at exposure times of 1–5 years (2004–2009) [16]. These values at each exposure time at the eight sites were standardized and then analyzed using PCA. Eigenvalues, proportion, cumulative proportion, and eigenvectors resulting from PCA are listed in Table 3.

Fig. 2 Outdoor exposure test at site 4

Table 3 Eigenvalue, proportion, cumulative proportion, and eigenvector calculated using the principal component analysis of climatic conditions

	PC1	PC2	PC3
Eigenvalue	2.34	0.477	0.186
Proportion (%)	77.9	15.9	6.19
Cumulative proportion (%)	77.9	93.8	100
Eigenvector			
T	0.605	−0.303	0.736
P	0.531	0.842	−0.090
S	0.593	−0.445	−0.671

Principal component analysis was conducted using the *T, P*, and *S* listed in Table 2. Prior to principal component analysis, the *T, P* and *S* were standardized

PC1 first principal component, *PC2* principal component, *PC3* third principal component, *T* annual mean temperature, *P* annual precipitation, *S* annual solar radiation

Prediction of CDI at eight sites using three RCP scenarios

To predict the future CDI at the eight sites in compliance with the three RCP scenarios, future temperature, precipitation, and solar radiation for 2031–2050 predicted with MIROC5 (Model for Interdisciplinary Research on Climate) were used [17]. MIROC5 predicted these climatic conditions of original spatial scales (about 125–444 km in latitude) in compliance with the three RCP scenarios. The original spatial scales were very large, so we interpolated these climatic conditions to the third mesh of the national standard grid system (about 1 km in latitude; 1 km × 1 km) using simple linear interpolation method [18]. The future CDI at the eight sites was then predicted using the developed PCA model that was described in "PCA using climatic conditions at eight sites" section in compliance with the three RCP scenarios.

Prediction of CDI nationwide using three RCP scenarios

To calculate the present CDI nationwide, the third mesh climatic conditions (temperature, precipitation, and solar radiation) from the Japan Meteorological Agency were used [19]. The third mesh of the national standard grid system (1 km × 1 km), which was described in "Prediction of CDI at eight sites using three RCP scenarios" section, was used to divide Japan's area; the area is 377,900 km^2, so we obtained 378,030 grid squares. Based on the future climatic conditions predicted with MIROC5, future temperature, precipitation, and solar radiation of 378,030 grid squares were spatially interpolated in compliance with the three RCP scenarios. The future CDI of the 378,030 grid squares was predicted using these climatic conditions in compliance with the three RCP scenarios.

Multiple regression analysis

The model used in multiple regression analysis was developed using the present CDI at the eight sites and the exposure time as explanatory variables. The criterion variable was the IB. The IB at the exposure time of 5 years at the eight sites was predicted using the developed multiple regression equation in relation to climate change occurring in compliance with the three RCP scenarios. The IB of the 378,030 grid squares nationwide at the exposure time of 5 years was also predicted using the developed model. IB retention was calculated using the following equation:

$$\text{IB retention (\%)} = \frac{\text{Predicted IB}}{\text{Initial IB before outdoor exposure test}} \times 100$$

Mapping

The distributions of the predicted IB at the exposure time of 5 years were mapped in compliance with the three RCP scenarios of the 378,030 grid squares using QGIS (version 2.2.0) (Geographic Information System).

Results and discussion

Solar radiation used to calculate CDI at eight sites

Solar radiation is generally preferable to sunshine duration for investigating the effects of sunshine on the IB reduction of particleboard. However, solar radiation was not measured at sites 2, 5, 6, and 8; only sunshine duration was measured. In our previous studies [9, 10], sunshine duration

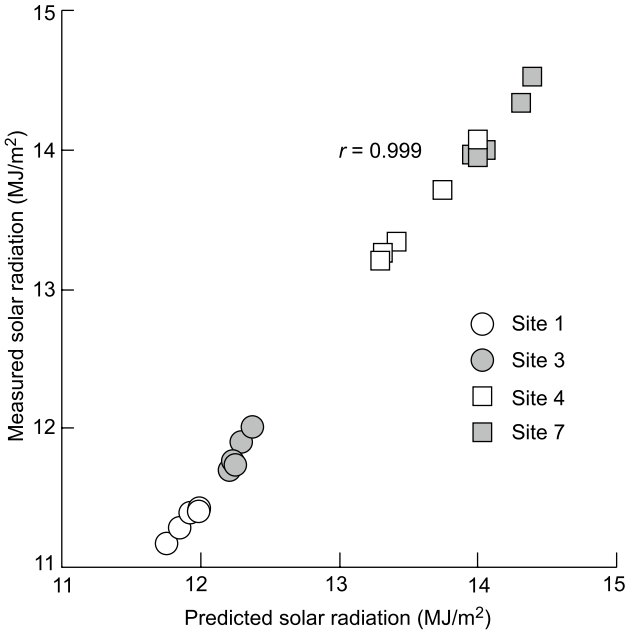

Fig. 3 Relationships between predicted and measured solar radiation at sites 1, 3, 4, and 7. Solar radiation at sites 2, 5, 6, and 8 was predicted using model that was developed by Kondo [12]. *r* correlation coefficient. Details about the sites are provided in Table 1

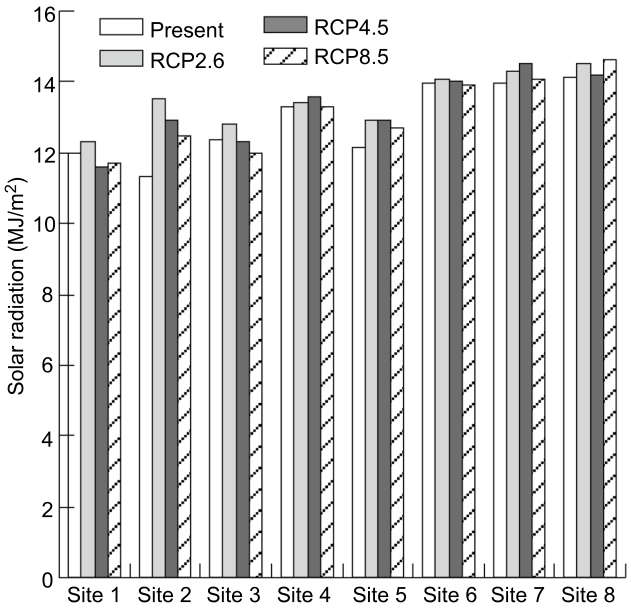

Fig. 5 Solar radiation change in compliance with three RCP scenarios, i.e., RCP2.6, RCP4.5, and RCP8.5, at eight sites. *RCP* representative concentration pathway. Details about the sites are provided in Table 1

was used to calculate the CDI. By contrast, in this study, solar radiation at sites 2, 5, 6, and 8 was predicted using the model that was developed to calculate the CDI [12].

Prior to using predicted solar radiation, the relationship between predicted solar radiation and measured solar radiation was investigated, and the accuracy of the model was confirmed. Solar radiation was measured at sites 1, 3, 4, and 7. Figure 3 shows the relationship between measured and predicted solar radiation at sites 1, 3, 4, and 7.

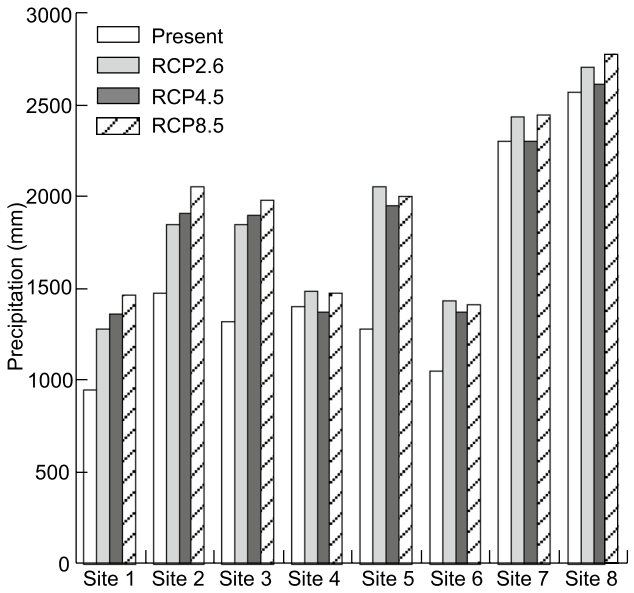

Fig. 4 Precipitation change in compliance with three RCP scenarios, i.e., RCP2.6, RCP4.5, and RCP8.5, at eight sites. *RCP* representative concentration pathway. Details about the sites are provided in Table 1

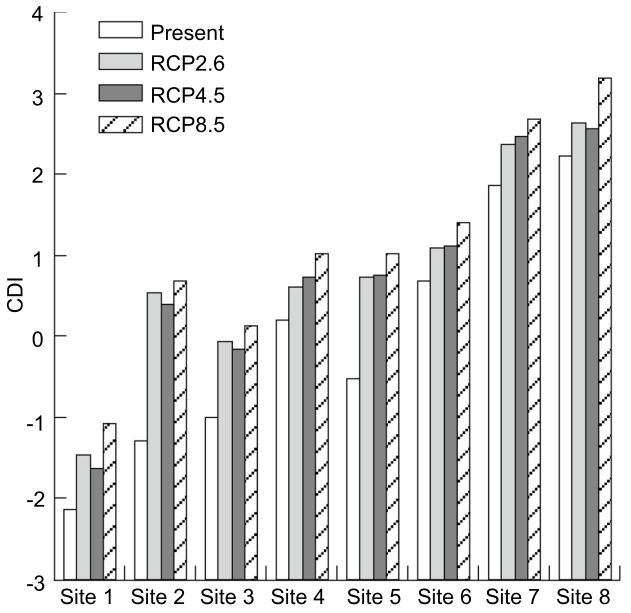

Fig. 6 CDI change in compliance with three RCP scenarios, i.e., RCP2.6, RCP4.5, and RCP8.5, at eight sites. *CDI* climate deterioration index, *RCP* representative concentration pathway. Details about the sites are provided in Table 1

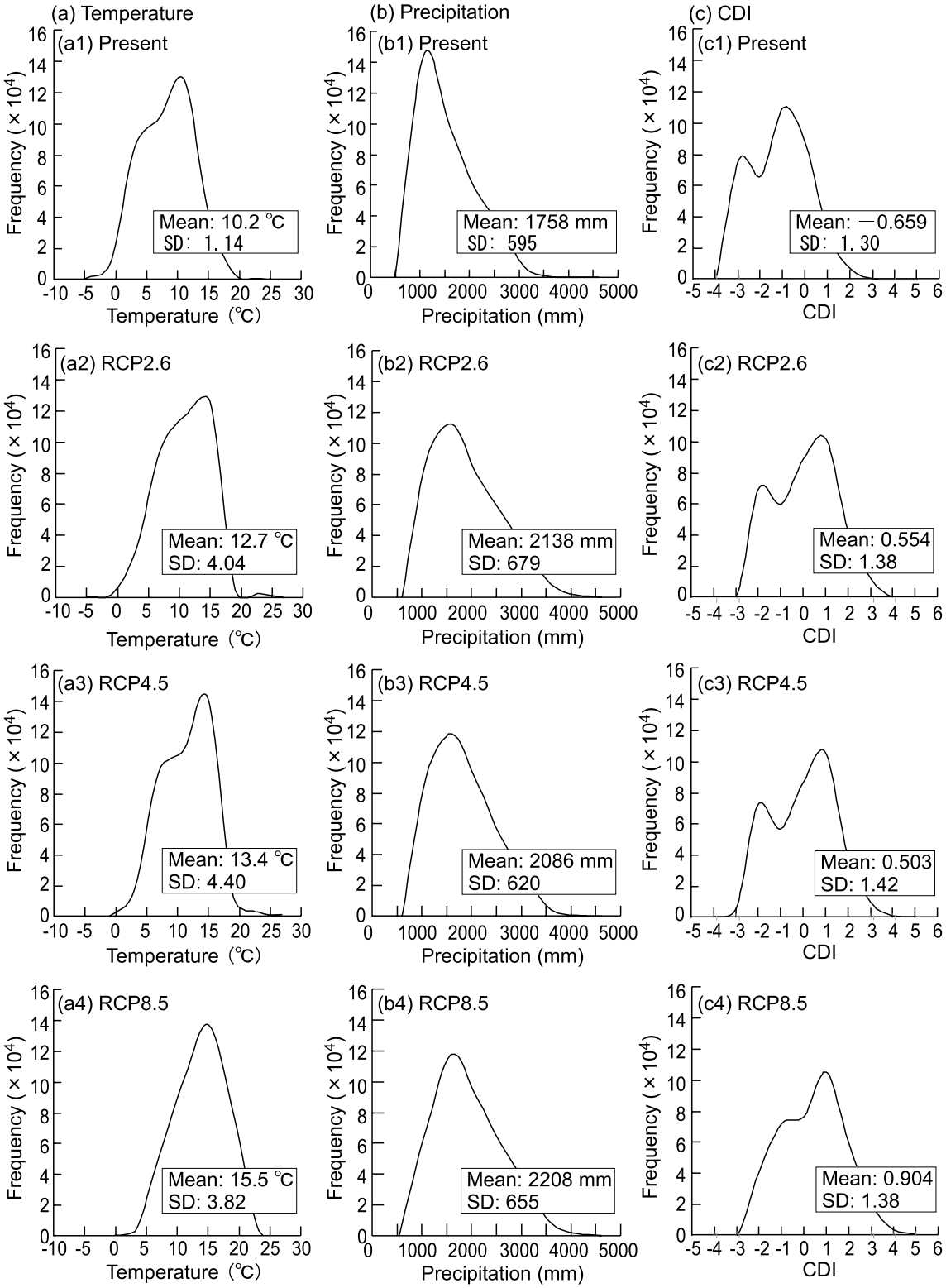

Fig. 7 Distribution changes in temperature, precipitation, and CDI of 378,030 grid squares in compliance with three RCP scenarios: RCP2.6, RCP4.5, and RCP8.5. *CDI* climate deterioration index. *RCP* representative concentration pathway, *SD* standard deviation

Table 4 Standardized regression coefficient, coefficient of determination, and adjusted coefficient of determination of the multiple regression equation

Standardized regression coefficient		R^2	Adjusted R^2
Exposure time	CDI		
−0.661***	−0.718***	0.857	0.850

***Statistical significance at 0.1% level. *CDI* climate deterioration index (score of first principal component). R^2 coefficient of determination. Adjusted R^2 adjusted coefficient of determination

The correlation coefficient was 0.999, showing a strong correlation between measured and predicted solar radiation. Thus, the model was able to predict solar radiation at sites 2, 5, 6, and 8, as listed in Table 2.

Table 3 lists the eigenvalue, proportion, cumulative proportion, and eigenvector calculated via PCA using temperature, precipitation, and solar radiation. For PC1, the eigenvalue was 2.34, and the proportion was 77.9%. These values indicated that 77.9% of the information relating to temperature, precipitation, and solar radiation was combined into PC1. Eigenvectors were used as coefficients to calculate the PC score. The PC1 score was calculated using the eigenvectors, and the equation is as follows:

$$\text{PC1 score (CDI)} = 0.605 \times T + 0.531 \times P + 0.593 \times S$$

T standardized annual temperature, P standardized annual precipitation, and S standardized annual solar radiation.

All eigenvectors of PC1 had positive values for each climatic condition, thereby indicating that the PC1 score increased with increasing temperature, precipitation, and solar radiation. These eigenvectors were almost equal, indicating that the PC1 score was equally affected by temperature, precipitation, and solar radiation. By contrast, the eigenvalues and proportions of PC2 and PC3 were significantly lower than those of PC1, suggesting that PC1 accounted for the majority of the variability caused by climatic conditions. Consequently, PC2 and PC3 scores were not used for analytical purposes in this study. As described in the "Introduction" section, the PC1 score was named the CDI, combined temperature, precipitation, and solar radiation into one explanatory variable. Thus, the CDI (PC1 score) was calculated using temperature, precipitation, and solar radiation at each exposure time (as listed in Table 2).

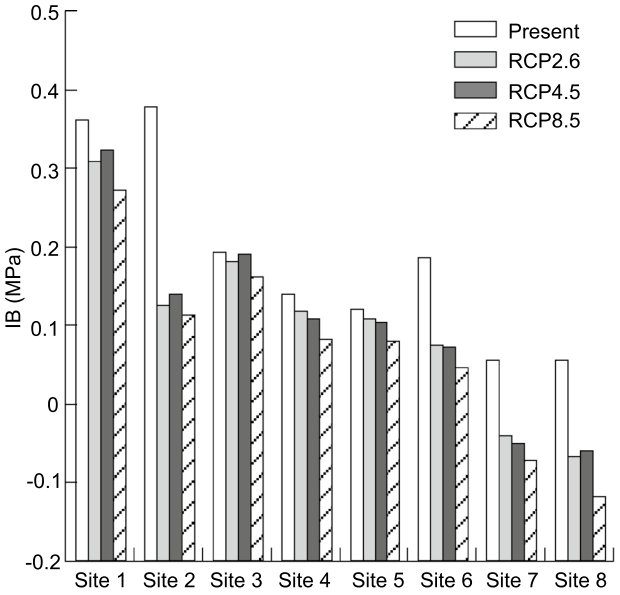

Fig. 8 IB change of particleboard subjected to 5-year outdoor exposure in compliance with three RCP scenarios, i.e., RCP2.6, RCP4.5, and RCP8.5, at eight sites. *IB* internal bond strength, *RCP* representative concentration pathway. Details about the sites are provided in Table 1

Climate change at eight sites

Figures 1, 4, and 5 show temperature, precipitation, and solar radiation changes in compliance with the three RCP scenarios at the eight sites, respectively. Temperature increased with increasing GHG emissions at all sites. The increasing rate of temperature at low-temperature sites was higher than that at other sites. Precipitation increased at low-temperature sites and sites 5 and 6. By contrast, solar radiation did not remarkably change at all sites with increasing GHG emissions. Figure 6 shows CDI change in compliance with the three RCP scenarios at the eight sites. The CDI mainly increased at all sites with increasing GHG emissions because of the rise in temperature.

Table 5 Analysis of variance table of multiple regression analysis of IB

Factor	Sum of squares	Degree of freedom	Mean square	F value	p value
Regression	1.44	2	0.722	111	2.24×10^{-16}***
Residual	0.240	37	0.00649		

IB internal bond strength

***Statistically significant at 0.1% level

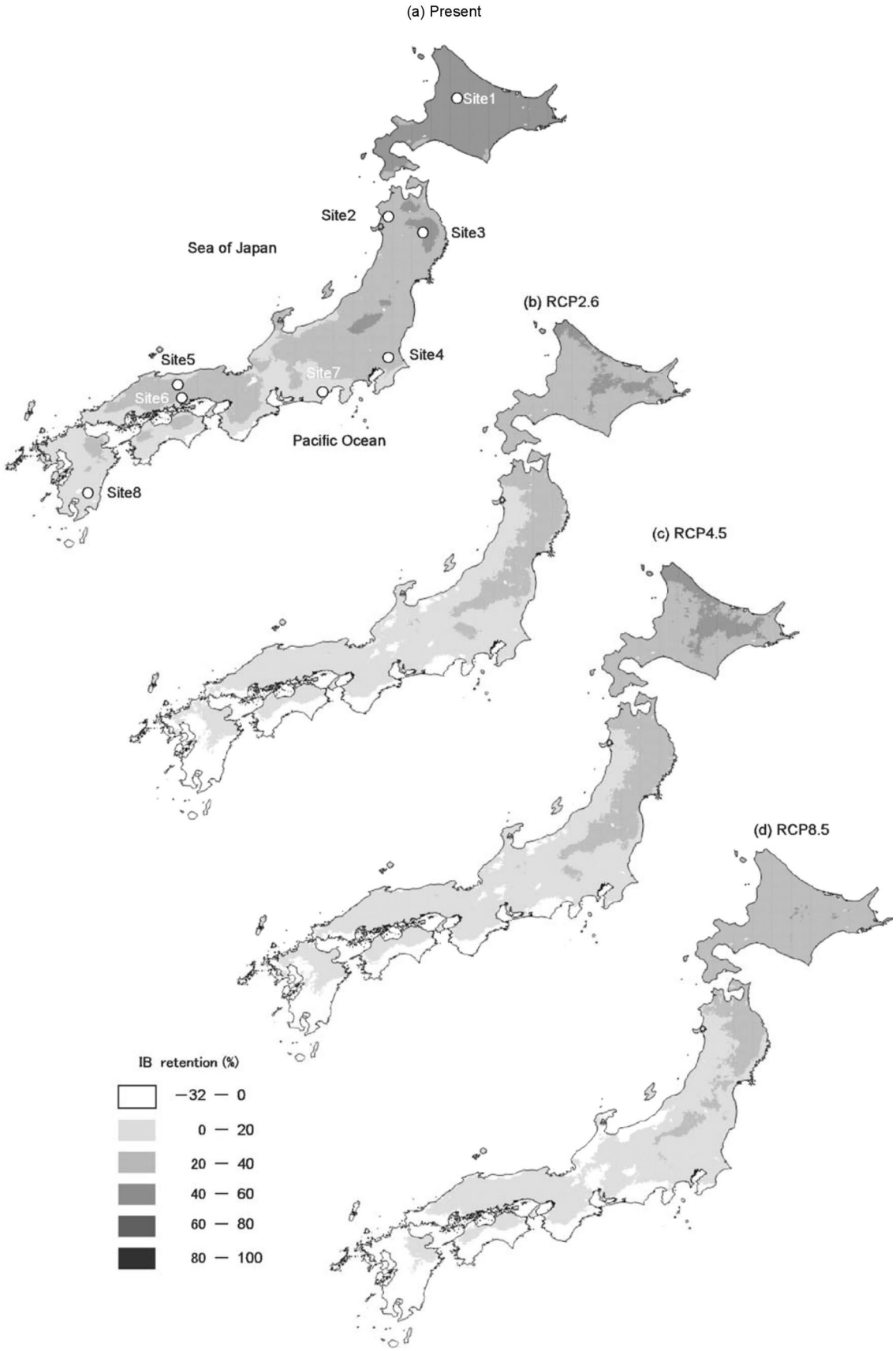
(a) Present
Site1
Site2
Site3
Sea of Japan
(b) RCP2.6
Site5
Site4
Site7
Site6
Pacific Ocean
Site8
(c) RCP4.5
(d) RCP8.5
IB retention (%)
−32 — 0
0 — 20
20 — 40
40 — 60
60 — 80
80 — 100

◂**Fig. 9** Map of IB retention predicted using multiple regression analysis model for the exposure time of 5 years of the 378,030 grid squares in compliance with the three RCP scenarios, i.e., RCP2.6, RCP4.5, and RCP8.5, at eight sites. *IB* internal bond strength, *RCP* representative concentration pathway

Distribution changes in temperature, precipitation, and CDI

Figure 7 shows the distribution changes in temperature, precipitation, and CDI of the 378,030 grid squares in compliance with the three RCP scenarios. As shown in Fig. 5, solar radiation did not considerably change at all sites, so the distribution change is not shown. The high peak of the present temperature distribution was approximately 10 °C, with a shoulder at the temperature range of 3–7 °C, as shown in Fig. 7a1. Compared with the present temperature distribution, high peaks in RCP2.6, RCP4.5, and RCP8.5 shifted from 10 to 15 °C, and the mean temperature increased from 10.2 to 15.5 °C. Furthermore, the shoulders of RCP2.6 and RCP4.5 shifted to the high-temperature range and that of RCP8.5 disappeared. A rise in temperature was observed throughout Japan, and the number of low-temperature areas decreased. As shown in Fig. 7b1–7b4, the high peak of the present precipitation distribution was approximately 1100 mm, but the peak shifted from 1100 to 1600 mm. No difference was noted among the distributions of RCP2.6, RCP4.5, and RCP8.5, and the mean precipitation of RCP2.6, RCP4.5, and RCP8.5 was almost the same. In Fig. 7c1, two peaks were found in the present CDI distribution at −3 and −1, and the peak at −3 was lower than that at −1. These peaks then shifted to a higher CDI in the RCP2.6 and RCP4.5 distributions with no difference between them. Furthermore, a shoulder and a peak, and not two peaks, were observed in the RCP8.5 distribution. High peaks were noted in the RCP2.6, RCP4.5, and RCP8.5 distributions, and these peaks shifted from −1 to 1 in comparison with the present CDI distribution. The mean CDI increased from −0.659 to 0.904 with increasing GHG emissions.

Multiple regression analysis of IB

Table 4 lists the standardized regression coefficient calculated using multiple regression analysis. The standardized regression coefficients of the exposure time and CDI were −0.661 and −0.718, respectively. Both values were negative and almost equal, indicating that the exposure time and CDI contributed to an equal IB reduction. Table 4 lists the coefficient of determination (R^2) and the adjusted coefficient of determination (adjusted R^2); both values were very high. Table 5 lists an analysis of variance table of the multiple regression analysis of the IB. The F value was very high, which was statistically significant at the 0.1% level. These results indicated that multiple regression analysis was able to accurately predict the IB.

Figure 8 shows the IB change of particleboard subjected to the exposure time of 5 years in relation to the three RCP scenarios at the eight sites using the developed multiple regression analysis model. The IB was found to decrease with increasing GHG emissions at all sites, and the reduction in high-temperature sites was higher than that in low- and middle-temperature sites. In particular, the IB at sites 7 and 8 significantly decreased. Climate change largely affected the IB reduction at high-temperature sites, and this reduction indicated other deterioration processes in particleboard because of outdoor exposure. The rupture of bonding points caused by outdoor exposure led to this reduction, and biodeterioration accelerated this reduction [20]. Particleboard was found to be prone to biodeterioration at high-temperature sites [21].

Although actual IB values were either positive or zero, the predicted IB showed negative values at sites 7 and 8 and was considered a null value. This finding was due to an assumption of linearity in multiple regression analysis, as discussed in the following section.

Map of IB reduction in Japan

Figure 9 shows a map of IB retention predicted using the multiple regression analysis model for the exposure time of 5 years of the 378,030 grid squares in compliance with the three RCP scenarios. At present, the IB reduction was large in the southern areas but small in the northern areas, and the reduction inland was smaller than that along the coastline. In particular, a large reduction was observed in the southern areas along the Pacific Ocean, which is a high-temperature area, and negative values were found for 8880 grid squares. IB retention in the 2.35% nationwide areas showed negative values. Negative IB retention in the high-temperature areas is related to the assumption of linearity in multiple regression analysis, which yields a null value. Therefore, in our previous study, we used an artificial neural network to solve this issue [6]. Low IB retention increased with increasing GHG emissions. For RCP8.5, the low IB retention areas significantly increased; the zone spread out along the Pacific Ocean side of western Japan and the Sea of Japan in central Japan. Negative IB retention was shown for 94,435 grid squares; IB retention in the 25% nationwide area showed negative values.

Conclusions

Temperature throughout Japan increased with increasing GHG emissions because of climate change. Therefore, the

CDI increased, and the number of low-temperature areas decreased. The rupture of bonding points caused by outdoor exposure led to IB reduction, and biodeterioration accelerated this reduction. In high-temperature areas, particleboard was significantly prone to biodeterioration. The low IB retention areas significantly increased with increasing GHG emissions; these areas spread out along the Pacific Ocean side of western Japan and the Sea of Japan in central Japan. Particleboards are difficult to use outdoors because of climate change. Negative IB retention in high-temperature areas is related to the assumption of linearity in multiple regression analysis, which yields a null value. This issue needs to be addressed using an artificial neural network or another method.

Acknowledgements This study was supported by a Grant-in-Aid for Scientific Research (21380108) from the Ministry of Education, Culture, Sports, Science and Technology of Japan and Social Implementation Program on Climate Change Adaptation Technology (SICAT). The authors are grateful for the Grants received. The authors would also like to thank Dr. Adachi of the Institute of Wood Technology, Akita Prefectural University, for predicting present solar radiation at sites 2, 5, 6, and 8. The outdoor exposure test was conducted as part of a project organized by the Research Working Group on Wood-based Panels from the Japan Wood Research Society. The authors sincerely thank all participants of this project.

References

1. Hann RA, Black JM, Blomquist RF (1962) How durable is particleboard? Forest Prod J 12:577–584
2. Gatchell CJ, Heebink BG, Hefty FV (1966) Influence of component variables on properties of particleboard for exterior use. Forest Prod J 16(4):46–59
3. River BH (1994) Outdoor aging of wood-based panels and correlation with laboratory aging. Forest Prod J 44(11/12):55–65
4. Suzuki S (2001) Evaluation of wood-based panel durability (in Japanese). Wood Industry 56: 7–12
5. Korai H, Sekino N, Saotome H (2012) Effects of outdoor exposure angle on the deterioration of wood-based board properties. Forest Prod J 62:184–190
6. Korai and Watanabe (2016) Predicting the strength reduction of particleboard subjected to various climatic conditions in Japan using artificial neural networks. Eur J Wood Prod. doi:10.1007/s00107-016-1056-8
7. Kojima Y, Shimoda T, Suzuki S (2012) Modified method for evaluating weathering intensity using outdoor exposure tests on wood-based panels. J Wood Sci 58:525–531
8. Sekino N, Sato H, Adachi K (2014) Evaluation of particleboard deterioration under outdoor exposure using several different types of weathering intensity. J Wood Sci 60:141–151
9. Korai H, Watanabe K (2015) Effectiveness of principal component analysis for analyzing particleboard subjected to outdoor exposure. J Wood Sci 61:35–39
10. Korai H, Watanabe K (2015) Comparison between climatic factors and climate deterioration index on strength reduction of particleboards subjected to various climatic conditions in Japan. Eur J Wood Prod 73:563–571
11. IPCC 2014. http://www.ipcc.ch/pdf/assessment-report/ar5/syr/AR5_SYR_FINAL_SPM.pdf. Accessed 23 March 2016
12. Kondo J (1994) Meteorology of the water environment—water and heat balance of the earth's surface (in Japanese). Asakura Shoten Press, Tokyo, p 348
13. JIS A 5908 (2003) JIS standard specification for particleboard. Japanese Standards Association, Tokyo
14. Korai H, Watanabe K, Nakao K, Matsui T, Hayashi T (2015) Mapping of strength reduction of particleboard subjected to various climatic conditions using a climate deterioration index. Eur J Wood Prod 73:807–817
15. R Core Team (2013) R: A language and environment for statistical computing. R Foundation for Statistical Computing, Vienna, Austria. http://www.R-project.org/ Accessed 12 January 2017
16. Japan Meteorological Agency. http://www.jma.go.jp/jma/index.html. Accessed 23 March 2016
17. MIROC5. http://www.icesfoundation.org/Pages/ScienceItemDetails.aspx?siid=181. Accessed 23 March 2016
18. Yokozawa M, Goto S, Hayashi Y, Seino H (2003) Mesh climate change impacts in Japan under the gradually increasing atmospheric CO_2 concentration. J Agric Meteorol 59:117–130
19. Japan Meteorological Business Support Center (2002) Mesh climatic data 2000 (in Japanese, CD-ROM). Japan Meteorological Agency
20. Korai H, Fujimoto Y (2015) Nail-head pull-through strength and lateral nail resistance strength of wood-based boards subjected to various climatic conditions in Japan. J Wood Sci 61:401–411
21. Brischke C, Rapp AO (2008) Dose-response relationships between wood moisture content, wood temperature and fungal decay determined for 23 European field test sites. Wood Sci Technol 42:507–518